ToxSci Advance Access published November 20, 2014

SOT Society of Toxicology
www.toxsci.oxfordjournals.org

TOXICOLOGICAL SCIENCES, 2014, 1–11

doi: 10.1093/toxsci/kfu235
Advance Access Publication Date: November 3, 2014

Downregulation of Stanniocalcin 1 is Responsible for Sorafenib-Induced Cardiotoxicity

Miko Kawabata[*,†,1], Noriko Umemoto[*,‡,1], Yasuhito Shimada[*,‡,§,¶,||], Yuhei Nishimura[*,‡,§,¶,||], Beibei Zhang[*], Junya Kuroyanagi[*], Masayuki Miyabe[†], and Toshio Tanaka[*,‡,§,¶,||,2]

[*]Department of Molecular and Cellular Pharmacology, Pharmacogenomics and Pharmacoinformatics, [†]Department of Clinical Anesthesiology, [‡]Department of Systems Pharmacology, Mie University Graduate School of Medicine, Mie 514-8507, Japan, [§]Mie University Medical Zebrafish Research Center, Mie 514-8507, Japan, [¶]Department of Bioinformatics, Mie University Life Science Research Center, Mie 514-8507, Japan and [||]Department of Omics Medicine, Mie University Industrial Technology Innovation, Mie 514-8507, Japan

[1]These authors contributed equally to this study

[2]To whom correspondence should be addressed at Department of Molecular and Cellular Pharmacology, Pharmacogenomics and Pharmacoinformatics, Mie University Graduate School of Medicine, 2-174 Edobashi, Tsu, Mie 514-8507, Japan. Fax: 81-59-232-1765. E-mail: tanaka@doc.medic.mie-u.ac.jp

ABSTRACT

Sorafenib is associated with adverse cardiac effects, including left ventricular dysfunction. However, the precise mechanism remains unclear. Here, we aimed to establish the genes responsible for this cardiotoxicity using zebrafish and human cardiomyocytes. Fluorescent cardiac imaging using pigmentless zebrafish with green fluorescent protein hearts revealed that the ventricular dimensions of the longitudinal axis with sorafenib were significantly shorter than those of the control group. Transcriptome analysis of their hearts revealed that stanniocalcin 1 (*stc1*) was downregulated by sorafenib. *stc1* knockdown in zebrafish revealed that reduction of *stc1* decreased the longitudinal dimensions of zebrafish ventricles, similar to that which occurs during sorafenib treatment. *STC1* downregulation and cytotoxicity were also seen in human cardiomyocytes exposed to sorafenib. To clarify the molecular function of *stc1* in sorafenib-induced cardiotoxicity, we focused on oxidative stress in cardiomyocytes treated with sorafenib. Reactive oxygen species (ROS) production significantly increased in both species of human cardiomyocytes and zebrafish exposed to sorafenib and *STC1* knockdown compared with the controls. Finally, we found that forced expression of *stc1* normalized impairment, decreasing the longitudinal dimensions in zebrafish treated with sorafenib. Our study demonstrated that STC1 plays a protective role against ventricular dysfunction and ROS overproduction, which are induced by sorafenib treatment. We discovered for the first time that *STC1* downregulation is responsible for sorafenib-induced cardiotoxicity through activated ROS generation.

Key words: sorafenib; stanniocalcin 1; cardiotoxicity; zebrafish; reactive oxygen species

Cardiotoxicity is one of the most significant adverse effects of cancer treatment, and is responsible for considerable morbidity and mortality (Adão *et al.*, 2013). Cardiac function is maintained by an intricate cycle of molecular signaling events that significantly overlap the signaling pathways of tumor growth. For example, many protein kinases are constitutively active in cancer cells, through mutations, overexpression, or translocation (Force *et al.*, 2007). However, the use of certain chemotherapeutics for the treatment of cancer is associated with a risk of adverse effects on cardiac function (Force *et al.*, 2007).

These kinase inhibitors can be cardiotoxic in a subset of patients (Force and Kolaja, 2011). With consideration to the therapeutic efficacy of these small molecular inhibitors, it is crucial to clarify the precise mechanism of drug-induced cardiotoxicity. Sorafenib is the first oral multikinase inhibitor that can inhibit v-raf-1 murine leukemia viral oncogene homolog 1 (RAF1), v-raf murine sarcoma viral oncogene homolog B1 (BRAF), fms-like tyrosine kinase (FLT)4, also known as vascular endothelial growth factor receptor (VEGFR)3, FLT3, v-kit Hardy-Zuckerman 4 feline sarcoma viral oncogene homolog (KIT), and platelet-derived growth factor receptor (PDGFR). The safety and efficacy of sorafenib in patients with advanced hepatocellular carcinoma (HCC) was demonstrated in two phase III randomized, double-blind, placebo-controlled trials, the Sorafenib HCC Assessment Randomized Protocol (SHARP) and Asia-Pacific (AP) trials (Cheng *et al.*, 2009; Llovet *et al.*, 2008b), thereby establishing sorafenib as the standard systemic therapy for advanced HCC (Bruix *et al.*, 2011; Llovet *et al.*, 2008a; Miyahara *et al.*, 2014). The left ventricular ejection fraction (LVEF) was found to be below the lower limit of normal at the time of “cardiac events” in 21.4% of patients, but the significance of this is entirely unclear because baseline LVEF was not determined. The study that examined baseline and serial LVEF determinations in patients on sorafenib reported that mean LVEF declined by only 0.8–1.2 EF percent (Cheng *et al.*, 2011; Tolcher *et al.*, 2011). These authors reported that the effects on LVEF were modest and were unlikely to be of clinical significance, but 13% of patients had significant declines in ejection fraction (EF) ($\geq$10 EF points). In the study by Schmidinger *et al.* (2008), the incidence of reduced LVEF for sorafenib was reported as 5%. Several mechanisms of sorafenib-induced cardiotoxicity have been reported, including inhibition of the RAF/mitogen-activated protein kinase kinase (MEK)/extracellular signal-regulated kinase (ERK) pathway (Cheng *et al.*, 2011; Mellor *et al.*, 2011), and disruption of VEGF-VEGFR signaling through inhibition of circulating VEGF and inhibition of PDGFRs (Hasinoff and Patel, 2010). Recently, Cheng *et al.* reported that sorafenib-induced cardiotoxicity may be preventable by activation of α-adrenergic signaling. Phenylephrine can activate ERK independently of RAF (Cheng *et al.*, 2011). Further studies are required to give more options for the prevention of sorafenib-induced cardiotoxicity.

Zebrafish have emerged as a useful animal model to clarify the molecular mechanisms of various cardiac diseases, including drug-induced cardiotoxicity (Lal *et al.*, 2013). Zebrafish in which a certain gene product associated with human heart failure was reduced, showed a decrease in EF, similar to the human phenotype (Seguchi *et al.*, 2007). We have also developed a fluorescent cardiac imaging of pigmentless zebrafish heart that can assess the cardiac function in various physiological and pathophysiological situations (Umemoto *et al.*, 2013). In this study, we applied functional cardiac imaging and transcriptome analysis to zebrafish to clarify the molecular mechanism of sorafenib-induced cardiotoxicity. These analyses, combined with the validation studies using human cardiomyocytes, revealed that downregulation of *STC1*, a gene that has cardioprotective function (Koizumi *et al.*, 2007; Liu *et al.*, 2012), is responsible for sorafenib-induced cardiotoxicity.

MATERIALS AND METHODS

This study was approved by the Ethics Committee of Mie University School of Medicine, Japan, and involved the use of zebrafish embryos as experimental animals. Animal care was also in accordance with the NIH guidelines.

Experimental animals. We obtained a pigmentless zebrafish line *nacre* (Lister *et al.*, 1999) from Zebrafish International Resource Center (ZIRC; Eugene, OR) and a transgenic zebrafish line SAG4A (Kawakami *et al.*, 2004) expressing enhanced green fluorescent protein (EGFP) in the heart from the National Institute of Genetics (Mishima, Japan). We crossed *nacre* and SAG4A to create MieKomachi 009 (MK009) (Supplementary Figure S1A). MK009 were bred and maintained as described by Westerfield (2007). Zebrafish were raised at 28.5 $\pm$ 0.5°C with a 14/10 h light/dark cycle. Embryos were obtained via natural mating and cultured in egg water (1.5 ml stock salts added to 1 l distilled water).

Sorafenib exposure. We filled a 6-well plate (Falcon, New York, NY) with 2 ml egg water per well (10 fish of 3 days post fertilization [dpf] in each of 6 baskets). Fifty zebrafish per group were analyzed. We administered sorafenib (1 or 3 μM) or 1% dimethyl sulfoxide (DMSO) to MK009 from 3 to 10 dpf, and changed the medium every day. MK009 were immobilized by placing them on 3% methylcellulose (Sigma-Aldrich, St. Louis, MO, USA) on a glass slide (Matsunami, Tokyo, Japan). Images were captured using a biological microscope (MZF16A; Leica, Wetzlar, Germany) with a digital camera (DP2; Olympus, Tokyo, Japan). The criterion for survival was the presence of cardiac contractions.

Cardiac imaging analysis. We administered 1 μM sorafenib or 1% DMSO to MK009 from 72 to 96 or 120 h post-fertilization (hpf). MK009 were immobilized by placing them on 3% methylcellulose in a microscopy chamber (u-Slide 8 well uncoated; ibidi, Munich, Germany) without anesthesia. After they were adjusted to a “head left” position, movie files were recorded on Image Xpress MICRO (Molecular Devices, Sunnyvale, CA, USA), at a frame rate of 33.5 frames/second for ~6 s.

We used MacBiophotonics Image J (NIH, Bethesda, MD) (Collins, 2007) to process the original records for the measurement of cardiac performance using GFP heart imaging, as described by Umemoto *et al.* (2013). To make M-mode images in the longitudinal (long) or short axes of the ventricle, the intersection of horizontal and vertical lines was positioned at the center of mass according to our preliminary experiment (Umemoto *et al.*, 2013). The ventricular end-systolic dimension (VDs) and the ventricular end-diastolic dimension (VDd) were measured from the M-mode images (Supplementary Figure S1B). VDs and VDd were obtained at maximal inward and outward excursions, respectively, of the ventricular wall in the M-mode images. We measured VDs and VDd along the short axis (short VDs and short VDd) and the longitudinal axis (long VDs and long VDd). For each determination, 5 diastoles and systoles were analyzed. The end-diastolic volume (EDV) and end-systolic volume (ESV) were calculated using the formula for a prolate spheroid ($4 \times a \times b^2/3$) (Jacob *et al.*, 2002). The stroke volume (SV) was obtained by subtracting the ESV from the EDV. The EF was calculated as SV/EDV and the percentage fractional shortening (FS) was calculated from the formula: 100 (short VDd – short VDs)/short VDd.

cDNA microarray analysis. MK009 treated with 1 μM sorafenib or 1% DMSO from 72 to 96 hpf were anesthetized using 0.05% 2 phenoxy-ethanol (Wako Pure Chemicals, Osaka, Japan). The hearts were surgically isolated using a fluorescence microscope. Twenty hearts were collected in a tube containing RNAlater (Life Technologies, Carlsbad, CA). Four biological replicates were prepared for each group. Total RNA was extracted using the RNAqueous-Micro Kit (Life Technologies), qualified by Agilent

Bioanalyzer 2100 (Agilent Technologies, Santa Clara, CA), and quantified using a spectrophotometer (Nano Drop ND-100; Wilmington, DE). In total, 700 of total RNA was converted into labeled cRNA using the Low Input Quick Amp Labeling Kit (Agilent Technologies). Cy3-labeled cRNA (1.65 μg) was hybridized to Agilent Zebrafish Whole Genome Oligo Microarrays (G2519F) according to the manufacturer's protocol. The hybridized microarrays were scanned by DNA Microarray Scanner (G2565BA; Agilent Technologies) and analyzed using Feature Extraction software (Agilent Technologies). The data were normalized using Agi4x44PreProcess. RankProd analysis was performed using Bioconductor to identify differentially expressed genes between two groups by calculating the false-discovery rate (FDR). Differentially expressed genes (FDR <10%) were then converted to human orthologs using the Life Science Knowledge Bank (World Fusion, Tokyo, Japan). These genes were subjected to Pathway Studio, which is a program used to visualize and analyze biological pathways and gene regulation networks. This program includes the ResNet database of >500 000 functional relationships between genes and and functional entities such as heart failure. The microarray dataset has been deposited in GEO as GSE61155.

Cell preparations. Human adult primary cardiomyocytes were purchased (PromoCell, Heidelberg, Germany) and cultured according to the manufacturer's instructions. Cardiomyocytes were grown for 2 weeks in a medium consisting of Myocyte Growth Medium Kit (PromoCell) supplemented with 5% fetal calf serum, epidermal growth factor (0.5 ng/ml), basic fibroblast growth factor (2 ng/ml), and insulin (5 μg/ml) at 37°C in a 5% CO_2 humidified incubator, and the medium was changed every day.

siRNA transfection. Stealth siRNAs (Stealth RNAi Negative Control Med GC [12935-300] and Stealth RNAi for STC1 [STC1siRNA1:HSS110297 and STC1siRNA2:HSS186139]) were purchased from Life Technologies, and were denoted as NCsiRNA and STC1siRNA1-2, respectively. Three biological replicates were prepared for each group. The sequences of siRNAs used in this study are shown in Supplementary Table S1. Cultured cells were transfected with siRNAs (50 nM final concentration) using Lipofectamine RNAiMAX (Life Technologies) according to the manufacturer's protocol.

Quantitative PCR Analysis. Total RNA from heart tissues and whole body of zebrafish was purified as described above. Total RNA from human cardiomyocytes was also purified using the RNeasy Mini Kit (Qiagen, Valencia, CA). First-standard cDNA was prepared with 200 ng total RNA and used to generate cDNA using an iScript Select cDNA Synthesis Kit (Bio-Rad, Hercules, CA). Quantitative polymerase chain reaction (qPCR) was performed using an ABI Prism 7300 (Life Technologies) with SYBR Green Real-time PCR Master Mix Plus (Toyobo, Osaka, Japan). The thermal cycling conditions comprised an initial step at 95°C for 1 min followed by 40 cycles of 95°C for 15 s, 60°C for 15 s and 72°C for 45 s. The sequences of primers used in this study are shown in Supplementary Table S1. Gene expression levels were calculated using the standard curve method.

Injections of morpholino and/or stc1 mRNA. The *stc1* antisense morpholino oligonucleotides (MOs) and standard control MO were purchased from Gene Tools (Philomath, OR). The *stc1* antisense MO was designed to splice out the second exon of *stc1* (zgc:153307). The sequences of MOs used in this study are shown in Supplementary Table S1.

The zebrafish *stc1* (amino acids 1–250) obtained from ZGC clone 153307 (Source BioScience, Nottingham, UK) was subcloned into the EcoRI and XbaI sites of the plasmid pCS2P+ (Addgene, Cambridge, MA). The sequence of the construct was confirmed by DNA sequencing (FASMAC, Kanagawa, Japan). The sequence containing full-length cDNA for *stc1* was amplified by PCR using the primer pairs: SP6 and T3. The PCR product was used as the template for RNA synthesis. The *stc1* mRNA was synthesized using the mMessage mMachine transcription kit for SP6 RNA polymerase (Life Technologies).

For knockdown of *stc1*, a solution containing 0.3 mM *stc1* MO was injected into 1- to 4-cell stage embryos. A solution containing 0.3 mM control MO was also injected into zebrafish as a control. For the rescue experiment, a solution containing mRNA (0.87 μM) with or without 0.3 mM *stc1* MO was injected into 1- to 4-cell stage embryos. These embryos were raised in egg water at 28.5°C until 96 hpf.

Reactive oxygen species measurement. In zebrafish experiments, we administered 1 μM sorafenib or 1% DMSO to MK009 from 72 to 74 hpf. DHE (Life Technologies) was dissolved in DMSO and used at a final concentration of 10 μM in egg water in the presence of 0.1% DMSO. Zebrafish were incubated with DHE for 15 min in the dark chamber (Ogrunc *et al.*, 2014), rinsed in egg water twice, and anesthetized using 2 phenoxy-ethanol, then immediately imaged under a Nikon stereomicroscope SMZ 25 (Tokyo, Japan) equipped with filters for DS-Red. Zebrafish fluorescent intensity of zebrafish whole body was quantified using the MacBiophotonics Image J (NIH).

Following 0.3 μM sorafenib or vehicle administration for 1 h, cultured cardiomyocytes were incubated with cell-permeable redox-sensitive fluorophore CellRox Deep Red detection reagent (Life Technologies) in a microscopy chamber (u-Slide 8 well uncoated; ibidi, Munich, Germany), at a concentration of 5 μM for 30 min. Hoechst 33342 dye (10 μM; Dojin, Kumamoto, Japan) was used to visualize the nuclei. Cardiomyocytes were washed with warm PBS twice. Cell images were acquired using Image Xpress MICRO high content screening system (Molecular Devices). Cell fluorescence was quantified using the accompanying software. Three biological replicates were prepared for each group. For determination of ROS, *N*-acetyl-cysteine (ENZO Life Science, Farmingdale, NY), a ROS scavenger, was used to cardiomyocytes at the concentration of 0.5 mM for 1 h prior to sorafenib administration.

Statistical analysis. Results are expressed as mean ± standard error. Differences among groups were tested for statistical significance using the unpaired Student's *t*-test, and $P < .05$ was considered significant. For multiple comparisons, one-way analysis of variance followed by the Tukey-Kramer procedure was used. All statistical analyses were conducted using Statcel 2 software (OMS, Tokyo, Japan).

RESULTS

Sorafenib Cardiotoxicity in Zebrafish line MK009

To assess the cardiotoxicity of sorafenib in zebrafish, we created a novel zebrafish line MK009 by crossing *nacre* and SAG4A. *nacre* is a zebrafish mutant with a pigmentless body due to lack of the *mitfa* gene (Lister *et al.*, 1999). SAG4A is a transgenic zebrafish in which GFP is selectively expressed in the heart (Kawakami *et al.*, 2004). MK009 is an attractive model for cardiac imaging, because the fluorescent heart can be clearly observed in the pigmentless body (Supplementary Figure S1A).

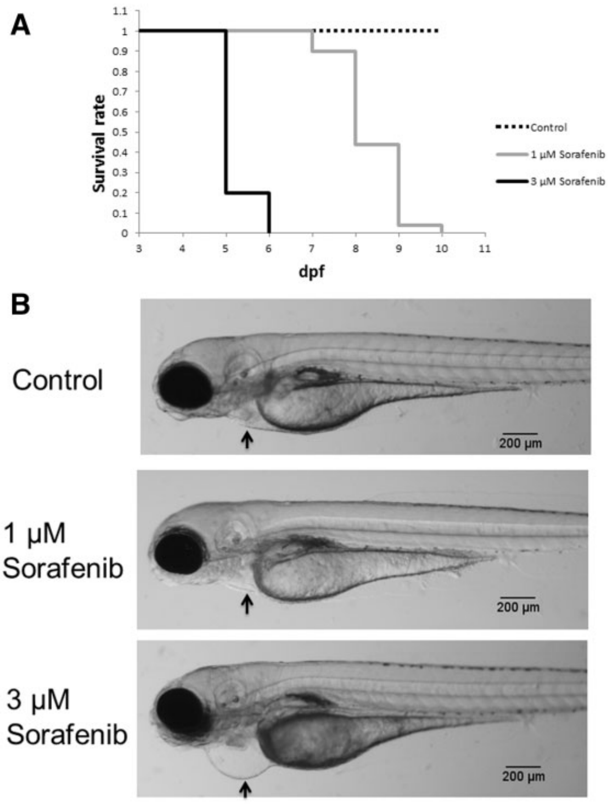

FIG. 1. Assessment of general toxicity of sorafenib in MK009 zebrafish. A, Survival rate of MK009 treated with or without sorafenib (1 or 3 μM) from 3 to 10 days post fertilization (dpf). Viable MK009 were counted daily from 3 dpf. Fifty zebrafish per group were analyzed. B, Treatment with 3 μM sorafenib from 72 to 96 hpf caused pericardial edema in MK009. MK009 treated with or without 1 μM sorafenib did not show pericardial edema or any external malformation. Scale bar: 200 μm.

The maximum plasma concentration of sorafenib after a 28-day cycle in patients receiving 400 mg, 2 times per day was 8.5 μM and the trough concentration was 6.4 μM in phase 1 clinical trials (Cheng, *et al.*, 2011; Strumberg, *et al.*, 2007; Tolcher, *et al.*, 2010). Thus, in the following experiments we choose the concentrations of 1 and 3 μM. The survival rate of zebrafish treated with 3 μM sorafenib was decreased by ∼20% at 5 dpf (Figure 1A, black solid line). In addition, zebrafish exposed to 3 μM sorafenib showed some noticeable body malformations including a curved body shape, and an uninflated swim bladder (Figure 1B). No zebrafish were alive in the 3 μM sorafenib group on 6 dpf. Zebrafish treated with 1 μM sorafenib did not show any decrease in survival rate until 6 dpf (Figure 1A, gray solid line) or any external malformation (Figure 1B) until 5 dpf.

We then assessed the cardiac function in zebrafish treated with 1 μM sorafenib using the quantitative fluorescent cardiac imaging that we have developed (Umemoto, *et al.* 2013) (Supplementary Figure S1B). As 3 μM sorafenib caused significant mortality by 120 hpf, 1 μM sorafenib was used for the remaining experiments. At 96 hpf (24-h exposure), both long VDd and VDs in zebrafish treated with sorafenib were significantly ($P < .05$) shorter than those of the control group (Figure 2A). However, the calculated EF and FS were not significantly different between zebrafish with sorafenib treatment and those of control group (Figure 2B). At 120 hpf (48 h exposure), long VDs in zebrafish treated with sorafenib were significantly ($P < .01$) longer than those of the control group (Figure 2C). Both the calculated EF and FS in zebrafish with sorafenib treatment were significantly ($P < .01$) decreased compared with the control group (Figure 2D). These results suggest that 1 μM sorafenib treatment from 72 to 96 hpf induced selectivity longitudinal impairment with preserved both EF and FS of zebrafish ventricle.

Sorafenib Reduces Expression of stc1 in Heart of MK009

To clarify the molecular mechanism of sorafenib-induced cardiotoxicity by eliminating the secondary effect of ventricular dysfunction, we performed transcriptome analysis of hearts isolated from zebrafish with or without exposure to 1 μM sorafenib for 24 h. Using a commercially available DNA microarray system, we analyzed the expression of 21 383 probes that were reliably expressed in the hearts (GSE 61155) and identified 215 genes significantly (false discovery rate; FDR <10%) dysregulated between hearts with and without sorafenib treatment (Supplementary Table S2). In total, 56 and 159 genes were significantly down- and upregulated, respectively, in the heart with sorafenib treatment.

To identify genes that might be relevant to sorafenib-induced cardiotoxicity, we performed a bioinformatics approach using the 215 genes dysregulated by sorafenib treatment in MK009 and Pathway Studio, a bioinformatics software. First, we selected "heart failure" as a functional entity in the Pathway Studio and identified 32 genes that were linked to heart failure (Supplementary Figure S2A). It has been shown that ERK (MAPK1 and MAPK3) are involved in sorafenib-induced cardiotoxicity (Cheng *et al.*, 2011; Hasinoff and Patel, 2010). Therefore, we selected "MAPK1" and "MAPK3" as molecular entities in the Pathway Studio and identified 14 genes whose expression was regulated by both MAPK1 (ERK2) and MAPK3 (ERK1) (Supplementary Figure S2B). Two and 12 genes were down- and upregulated in the hearts with sorafenib treatment, respectively. It has been reported that sorafenib inhibits the phosphorylation of MAPK1 and MAPK3 and the function of these ERKs. We focused on *stc1* because the expression of *stc1* was positively regulated by ERK (Nguyen *et al.*, 2009) and VEGF (Holmes and Zachary, 2008) signaling. We performed qPCR to confirm the downregulation of *stc1* in the hearts of zebrafish exposed to sorafenib. As shown in Figure 3A, the expression level of *stc1* was significantly ($P < .05$) lower than that of the control heart.

We performed qPCR to confirm the downregulation of *STC1* exposed to 0.3 μM sorafenib or vehicle for 24 h. As shown in Figure 3B, the expression level of *STC1* in human cardiomyocytes exposed to sorafenib was significantly ($P < .05$) lower than that exposed to the vehicle.

Reduction of stc1 Impairs Cardiac Function in MK009

We examined whether the reduction of *stc1* affected cardiac function in MK009. To knock down *stc1* expression, zebrafish embryos were injected with *stc1* MO. We conducted *stc1* knockdown using splicing inhibitor MO, and confirmed the gene knockdown level by qPCR. ($P < .01$ sorafenib vs vehicle, Figure 3C). Functional cardiac imaging at 96 hpf revealed that both long VDs and long VDd in *stc1* morphant (Figure 3D, black bar) were significantly shorter than those in control zebrafish that were injected with control MO (Figure 3D, white bar). The calculated EF and FS were not significantly different between *stc1* morphant and control zebrafish (Figure 3E). The reduction of both long VDs and long VDd in *stc1* morphant at 96 hpf was similar to that in zebrafish exposed to sorafenib from 72 to 96 hpf (Figure 2A).

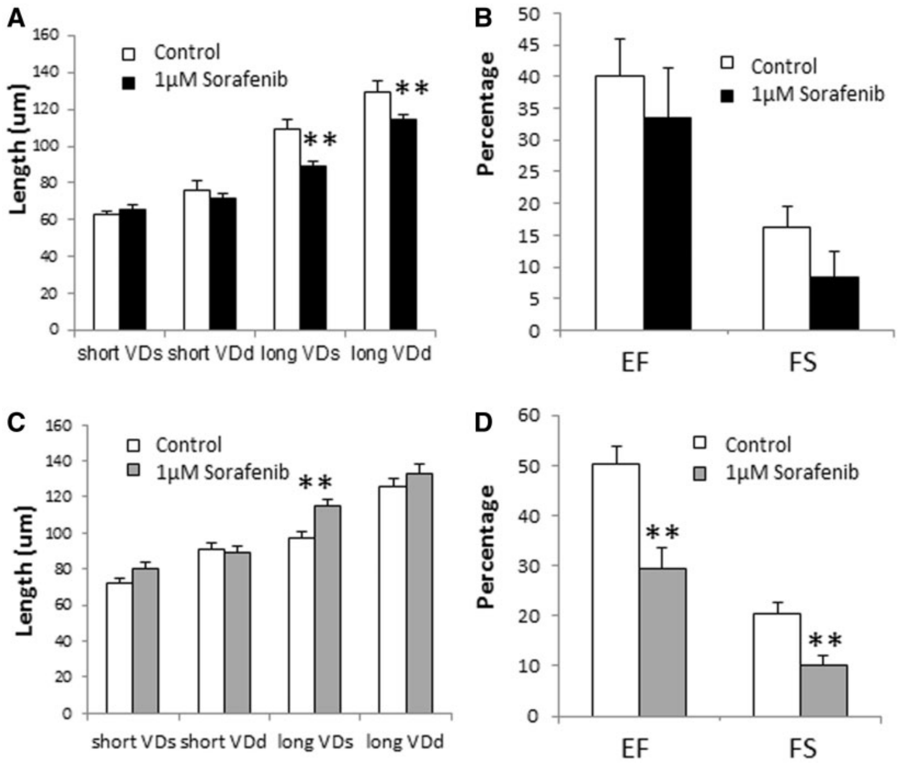

FIG. 2. Sorafenib cardiotoxicity in MK009 zebrafish. MK009 were treated with or without 1 μM sorafenib from 72 to 96 or 120 hours post-fertilization (hpf). Functional cardiac imaging was performed at 96 or 120 hpf. A, Assessment of ventricular end-systolic dimension (VDs) or ventricular end-diastolic dimension (VDd) of both short and long axes at 96 hpf. B, Calculated ejection fraction (EF) and fractional shortening (FS) based on VDd and VDs at 96 hpf. A, B, control, $n = 9$; sorafenib, $n = 13$; $^{**}P < .01$. C, Assessment of VDs or VDd of both short and long axes at 120 hpf. D, Calculated EF and FS based on VDd and VDs at 120 hpf. C, D, control, $n = 10$; sorafenib, $n = 12$; $^{**}P < .01$.

To confirm whether the decrease in long VDs and long VDd in *stc1* morphant was caused by reduced expression of *stc1*, zebrafish embryos were co-injected with *stc1* MO and *stc1* mRNA. *stc1* MO was designed to bind to the junction of the first intron and second exon of *stc1*, thus *stc1* MO was not likely to bind to *stc1* mRNA. Therefore, *stc1* mRNA should be translated into *stc1* protein without interference from *stc1* MO. Functional cardiac imaging at 96 hpf revealed that both long VDs and long VDd were significantly increased in zebrafish co-injected with *stc1* MO and *stc1* mRNA (Figure 3D, gray bar) compared with those of *stc1* morphant (Figure 3D black bar). The calculated EF and FS were not statistically different among the three groups (Figure 3E). These results suggest that reduction of *stc1* could cause dysregulation of ventricular dimensions in zebrafish.

Sorafenib-Induced STC1 Reduction Causes ROS Overproduction in Human Cardiomyocytes

It has been reported that sorafenib increases ROS generation in human cancer cells (Coriat *et al.*, 2012; Fumarola *et al.*, 2013) and that *STC1* suppresses ROS generation induced by angiotensin II in rodent cardiomyocytes (Liu *et al.*, 2012). To examine the relationship between *stc1* and cardiotoxicity, we observed accumulation of ROS throughout the body of zebrafish treated with 1 μM sorafenib for 2 h (Figure 4A). ROS were detected *in vivo* by adapting a protocol based on DHE. ROS generation of zebrafish treated with sorafenib was significantly increased in vehicle-treated zebrafish (Figure 4B). NAC, a known scavenger of ROS, inhibited the increase in ROS level by sorafenib treatment (Figure 4B). To examine whether reduction of *stc1* affected ROS generation, zebrafish embryos were injected with 0.3 mM *stc1* MO or 0.3 mM control MO (Figure 4C). ROS generation was significantly increased in zebrafish injected with *stc1* MO compared with control MO (Figure 4D and E) and with *stc1* MO + *stc1* mRNA (Figure 4E).

Furthermore, to validate the involvement of *STC1* in sorafenib-induced cardiotoxicity in humans, we conducted an *in vitro* study using human cardiomyocytes. To examine whether sorafenib induces ROS generation in cardiomyocytes, we treated human cardiomyocytes with or without 0.3 μM sorafenib for 1 h and assessed the ROS generation using fluorescent imaging. As shown in Figure 5A and B, ROS generation was significantly ($P < .05$) increased in human cardiomyocytes exposed to sorafenib compared with that in the control. To examine whether reduction of *STC1* could affect ROS generation, human cardiomyocytes were transfected with *STC1* or negative control (NC) siRNA. ROS generation was significantly ($P < .05$) increased in human cardiomyocytes transfected with STC1siRNA compared with NC siRNA (Figure 5C and D). As shown in Figure 5E, the expression of *STC1* in human cardiomyocytes transfected with STC1siRNA were significantly ($P < .05$) lower than that of NCsiRNA.

Forced Expression of stc1 Reverses Sorafenib-Induced Cardiotoxicity

We investigated whether forced expression of *stc1* reversed sorafenib-induced cardiotoxicity in zebrafish. Zebrafish embryos were injected with or without *stc1* mRNA and treated with or without 1 μM sorafenib from 72 to 96 hpf. Functional cardiac imaging at 96 hpf revealed that both long VDs and long VDd in zebrafish without *stc1* mRNA injection and with sorafenib treatment (Figure 6A, black bar) were significantly shorter than

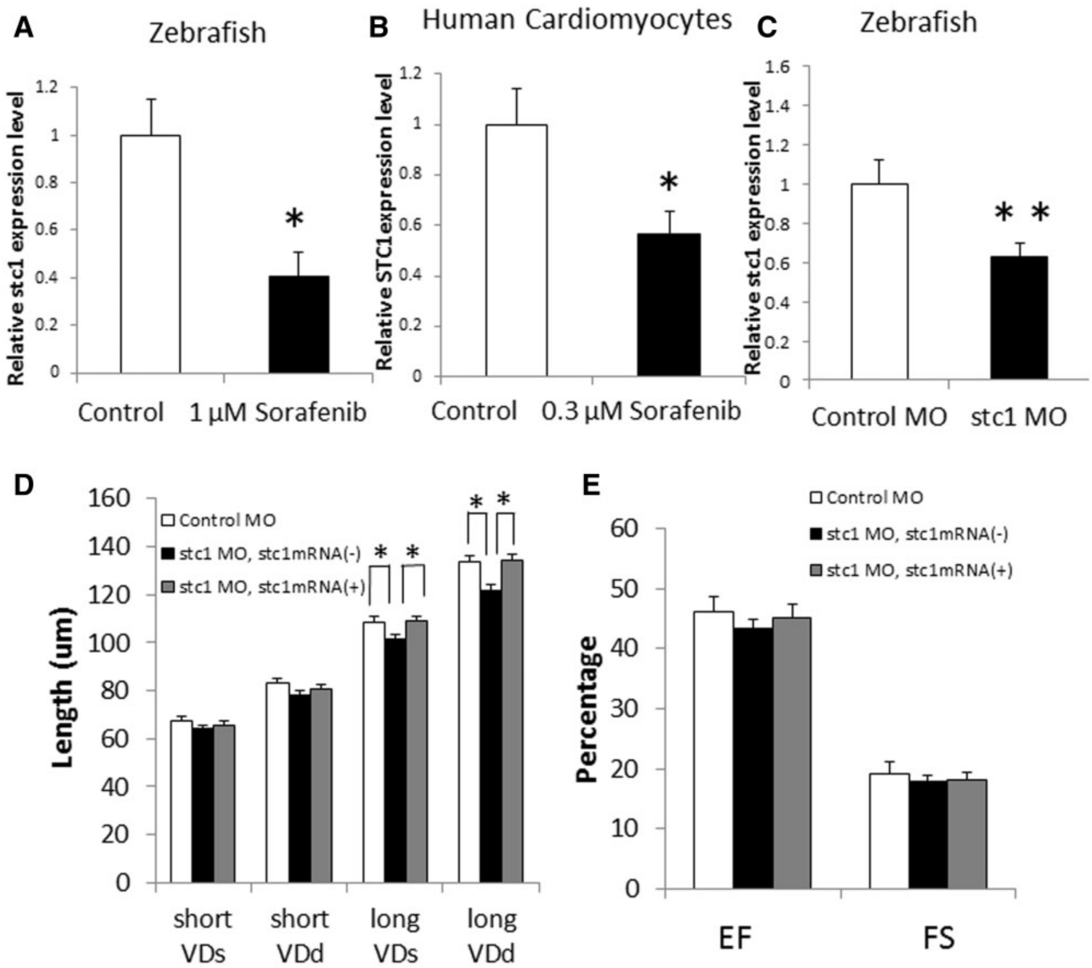

FIG. 3. Reduction of *stc1* expression caused a significant decrease in ventricular dimension. A, B, quantitative polymerase chain reaction (qPCR) to assess *stc1* (*STC1*) expression. A, MK009 were treated with or without 1 μM sorafenib from 72 to 96 hours post-fertilization (hpf). The hearts were isolated from these zebrafish and qPCR was performed to assess the expression of *stc1*.*P < .05, zebrafish treated with sorafenib versus zebrafish without sorafenib treatment. Four samples per group were analyzed. One sample contained 20 hearts of zebrafish. B, Human cardiomyocytes were treated with or without 0.3 μM sorafenib for 24 h. qPCR was performed to assess the expression of *STC1*. *P < .05. Four samples per group were analyzed. C, MK009 at 1- to 4-cell stages were injected with 0.3 mM *stc1* morpholino oligonucleotides (MOs) and raised to 96 hpf. Total RNA was extracted from the whole body and qPCR was performed to assess expression of *stc1*. **P < .01, zebrafish injected with *stc1* MO versus zebrafish injected with control MO. Eight zebrafish per group were analyzed. D, E, Assessment of cardiac function in zebrafish injected with control MO, *stc1* MO or *stc1* MO and *stc1* mRNA. Twenty zebrafish per group were analyzed. For multiple comparisons, one-way analysis of variance followed by the Tukey-Kramer procedure was used. D, Assessment of ventricular end-systolic dimension (VDs) or ventricular end-diastolic dimension (VDd) of both short and long axes. E, Calculated ejection fraction (EF) and fractional shortening (FS) based on VDd and VDs. *P < .05

those in zebrafish without *stc1* mRNA and sorafenib (Figure 6A, white bar) and zebrafish with *stc1* mRNA and without sorafenib (Figure 6A, gray bar). Both long VDs and long VDd in zebrafish with *stc1* mRNA injection and sorafenib treatment (Figure 6A, shaded bar) did not differ significantly from those in zebrafish without *stc1* mRNA and sorafenib (Figure 6A, white bar). There was no significant difference in the calculated EF and FS among the 4 groups (Figure 6B). Furthermore, forced expression of *stc1* mRNA suppressed sorafenib-induced ROS generation (Figure 6C). These results suggest that reduction of *stc1* could be responsible for sorafenib-induced cardiotoxicity.

DISCUSSION

The pigmentless zebrafish line MK009 was developed to allow quantitative observation of heart function that is highlighted by GFP. Owing to fluorescent cardiac image analysis of MK009, using a high-content imager with LED illumination as an inverted fluorescent microscope, we were able to demonstrate that the ventricular dimension of the longitudinal axis decreased with preserved EF and FS in zebrafish treated with 1 μM sorafenib from 72 to 96 hpf. This cardiac functional imaging is an innovative way to detect clearly the target tissues, if the intensity of fluorescence in the tissues is as weak as that of cardiac GFP in MK009, because the LED illumination of the high-content imager is brighter than the halogen illumination of simple manual microscopes. We also found that the longitudinal dimension increased with reduced EF and FS in zebrafish treated with 1 μM sorafenib from 72 to 120 hpf (Figure 2D). These results were consistent with a previous study that reported a significant increase in the end-systolic dimension of both ventricular axes and decreased FS after administration of 0.5 μM sorafenib from 48 to 120 hpf (Cheng *et al.*, 2011). In a previous clinical study, a reduction in the ventricular dimension of the longitudinal axis was detected in patients with early-stage heart failure induced by sorafenib (Di Salvo *et al.*, 2011). This is in good agreement with our study that showed reduced longitudinal

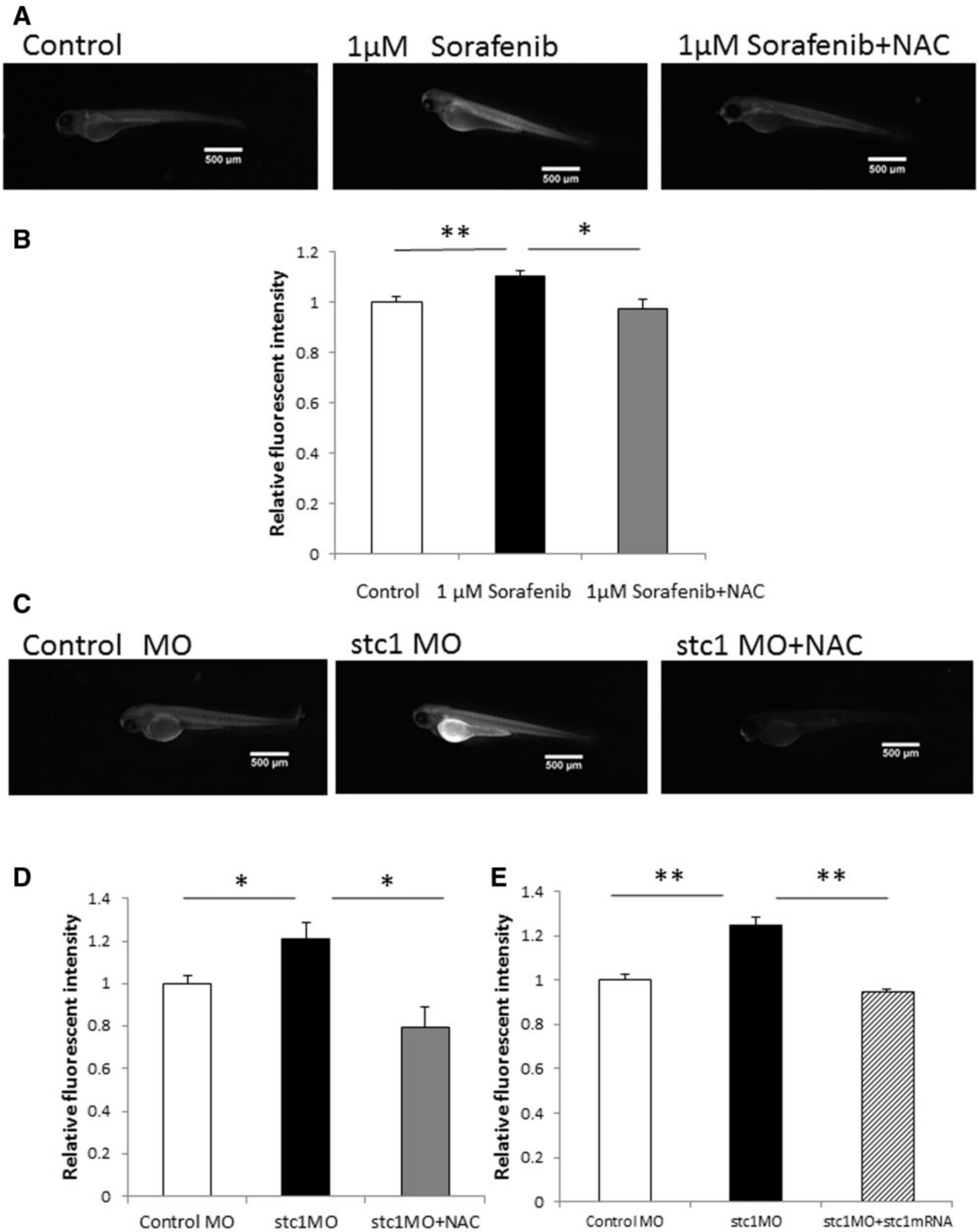

FIG. 4. Reactive oxygen species (ROS) overproduction in zebrafish treated with sorafenib, or injected with *stc1* morpholino oligonucleotides (MO). ROS was detected using dihydroethidium (DHE). Images were performed at 74 hpf. A, Typical images of zebrafish treated with vehicle, 1 μM sorafenib, 1 μM sorafenib + 5 mM NAC for 2 hours. Scale bar: 500 μm. (*B*) Quantitative analysis of ROS in the zebrafish. (n = 15), $^{*}P < 0.05$, $^{**}P < 0.01$. (C) Typical images of zebrafish injected with 0.3 mM control MO, 0.3 mM *stc1* MO, 0.3 mM *stc1* MO + 5 mM NAC. Scale bar: 500 μm. D, Quantitative analysis of ROS in the zebrafish. (Control MO, $n = 8$; *stc1* MO, $n = 10$; *stc1* MO + NAC, $n = 6$), $^{*}P < .05$. E, Quantitative analysis of ROS in the zebrafish injected with 0.3 mM control MO, 0.3 mM *stc1* MO, 0.3 mM *stc1* MO + *stc1* mRNA ($n = 10$), $^{**}P < .01$.

dimension in zebrafish treated with sorafenib from 72 to 96 hpf. These results suggest that the zebrafish cardiotoxic model treated with 1 μM sorafenib for 24 h showed selective longitudinal ventricular dysfunction with preserved EF and FS, which mimicked sorafenib-induced cardiotoxicity in humans.

To establish the mechanism of cardiotoxicity as on-target and off-target effects, we aimed to identify differentially expressed genes in the sorafenib-induced cardiotoxic model. Sorafenib inhibited RAF1, which is coded by mitogen activated protein kinase kinase kinase (MAP3K). Once activated, RAF1 can phosphorylate the dual specificity protein kinases MEK1/2 to activate them. These in turn phosphorylate the serine-/threonine-specific protein kinases ERK1/2 to activate them (Roux and Blenis, 2004). Activated ERKs are effectors of cell physiology and control gene expression involved in the regulation of cell cycle progression, proliferation, cytokinesis, transcription,

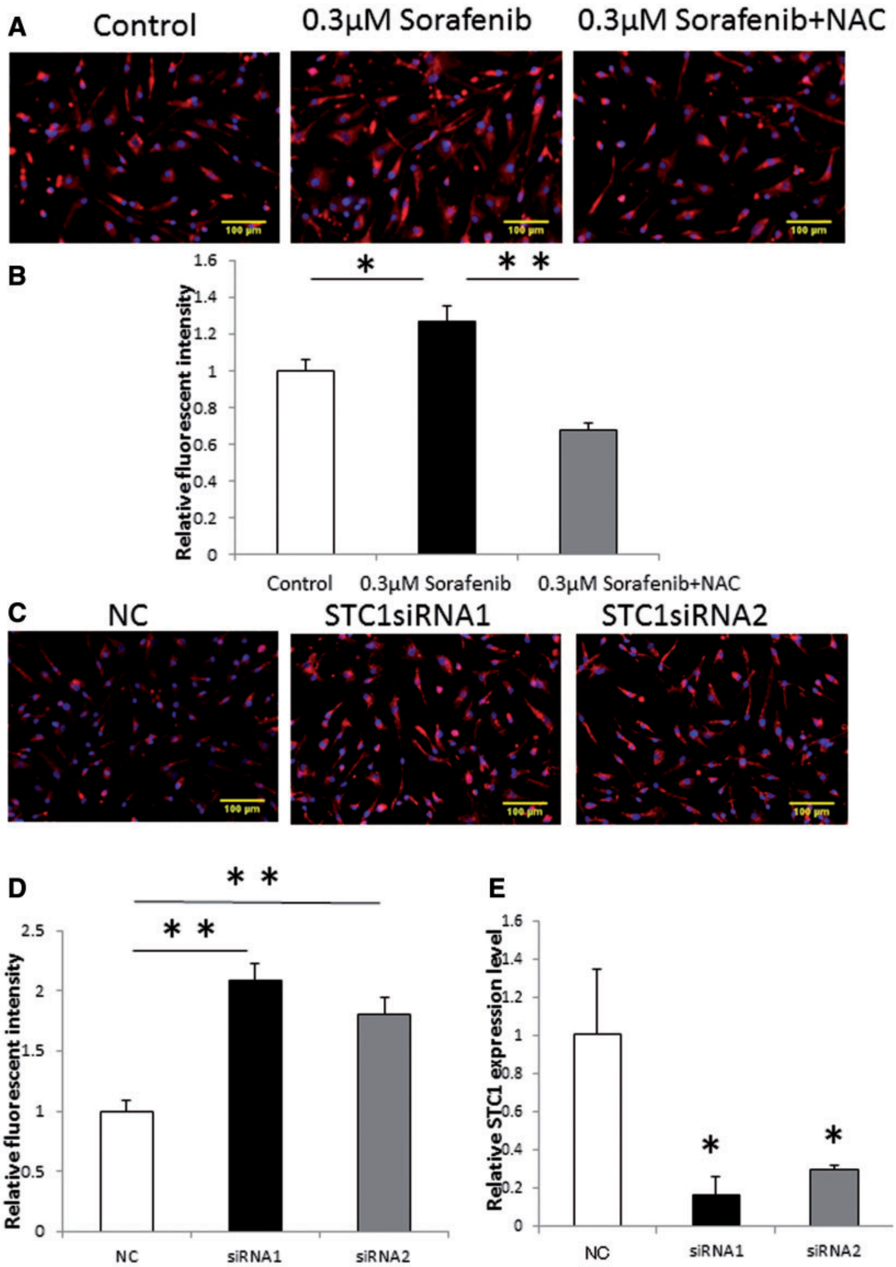

FIG. 5. Reactive oxygen species (ROS) overproduction in human cardiomyocytes treated with sorafenib, or transfected with STC1siRNA. 'ROS was detected using CellRox dyes.' in black and white. A, Typical images of cardiomyocytes treated with vehicle, 0.3 μM sorafenib, 0.3 μM sorafenib + 5 mM NAC for 1 h. Scale bar: 100 μm. B, Quantitative analysis of ROS in the cells. (control, $n = 8$; sorafenib, $n = 8$; sorafenib + NAC, $n = 5$), $^{*}P < .05$, $^{**}P < .01$. C, Typical images of cardiomyocytes transfected with NC siRNA and STC1siRNAs. Cultured cells were transfected with siRNAs. Scale bar: 100 μm. D, Quantitative analysis of ROS in the cells. ($n = 4$), $^{**}P < .01$. E, Human cardiomyocytes were transfected with NCsiRNA and STC1siRNAs. Quantitative polymerase chain reaction (qPCR) was performed to assess expression of *STC1*. $^{*}P < .05$, cardiomyocytes with STC1siRNA versus cardiomyocytes with negative control. Three samples per group were analyzed.

differentiation, senescence, and apoptosis (Orphanos *et al.*, 2009). RAF1 inhibits two proapoptotic kinases, apoptosis signal-regulating kinase (ASK)1 and mammalian sterile 20-like kinase (MST)2, which are important in oxidative-stress-induced injury. Deletion of RAF1 gene in the heart leads to a dilated, hypocontractile heart with increased cardiomyocyte apoptosis (Feng *et al.*, 2013).

In this study, to determine an accurate gene expression profile in the sorafenib-induced cardiotoxic model, we performed transcriptome analysis using a cDNA microarray from a small amount of heart tissue (20 hearts per group). In a previous transcriptome analysis of heart tissue in zebrafish (Burns and MacRae, 2006), the authors used 500 isolated hearts of zebrafish larvae for each condition of their microarray experiment. However, their technology for heart isolation using a micropipette carries a risk of including noncardiac tissue in the samples. In our study, we developed a method to isolate cardiac tissue easily from zebrafish larvae by using microsurgical scissors and preparing RNA samples extracted from 20 hearts for each DNA chip. We analyzed the expression data using Gene Set Enrichment Analysis (GSEA) by Pathway Studio to find gene ontology (GO) associated with the 215 genes whose expression

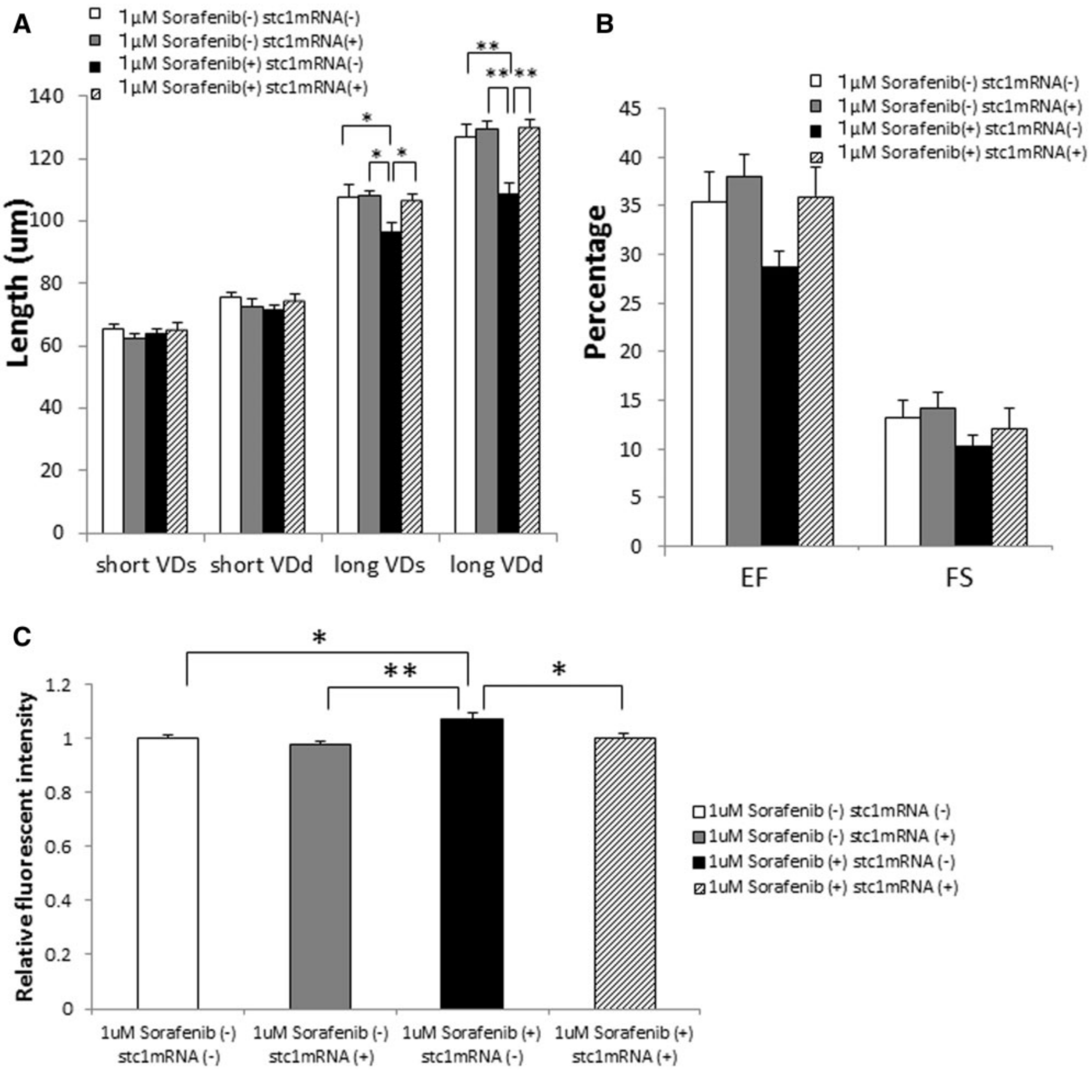

FIG. 6. Forced expression of *stc1* mRNA reversed sorafenib-induced cardiotoxicity. A, B, MK009 zebrafish at 1- to 4-cell stages were injected with or without *stc1* mRNA and treated with or without 1 μM sorafenib from 72 to 96 hpf. Functional cardiac imaging was performed at 96 hpf. A, Assessment of VDs or VDd of both short and long axes. B, Calculated ejection fraction (EF) and fractional shortening (FS) based on ventricular end-systolic dimension (VDs) and ventricular end-diastolic dimension (VDd). Seventeen zebrafish per group were analyzed. *$P < .05$, **$P < .01$. C, Quantitative analysis of reactive oxygen species (ROS) in the zebrafish. MK009 zebrafish at 1- to 4-cell stages were injected with or without *stc1* mRNA and treated with or without 1 μM sorafenib from 72 to 74 hpf. Thirteen zebrafish per group were analyzed. *$P < .05$, **$P < .01$. A, B, C, For multiple comparisons, one-way analysis of variance followed by the Tukey-Kramer procedure was used.

levels were altered by sorafenib treatment in zebrafish. From the DNA microarray analysis, we identified 14 genes whose expression was regulated by both MAPK1 and MAPK3, and was linked to heart failure using a bioinformatics approach of Pathway Studio. Two and 12 genes were down- and upregulated in the hearts with sorafenib treatment, respectively (Supplementary Figure S2B).

We focused on oxidative stress as a potential off-target effect of sorafenib. It is known that sorafenib can provoke rapid generation of various ROS in two HCC cell lines (HepG2 and Hepa 1.6) and human umbilical vein endothelial cells, and exerts dose-dependent cytostatic and cytotoxic effects (Chiou *et al.*, 2009; Jacob *et al.*,2002). Additionally, it is recognized that anticancer agents, such as adriamycin, induce dose-limiting cardiotoxicity. There is a consensus that this toxicity is related to the induction of ROS. Induction of ROS in the heart by adriamycin occurs via redox cycling of the drug at complex I of the electron transport chain (Berthiaume and Wallace, 2007). We hypothesized that sorafenib might induce the overproduction of ROS in the heart. In fact, Hasinoff and Patel (2010) reported that sorafenib treatment of neonatal rat cardiomyocytes caused dose-dependent damage and increased oxidative activity at therapeutically relevant concentrations . A previous clinical study also reported that serum levels of advanced oxidation protein products on ROS in patients with HCC treated with sorafenib were increased after 15 days treatment (Coriat *et al.*, 2012). However, these authors could not clarify the mechanism of sorafenib-induced cardiotoxicity. As a result of the GSEA in our study, *STC1* was classified in "ROS generation" in the GO list of cell processing categories (Supplementary Table S3). To the best of our knowledge, this is the potential mechanism of sorafenib-induced cardiotoxicity. Here, we demonstrated overproduction of ROS and reduction of *stc1* in zebrafish treated with 1 μM sorafenib for 2 and 24 h, respectively. Overproduction of ROS and reduction of *STC1* in human cardiomyocytes treated with 0.3 μM sorafenib for 1 h were also shown in our study. We also observed a cytotoxic phenotype in human cardiomyocytes treated with 1 μM sorafenib for 24 h (data not shown). Moreover, *STC1* knockdown in zebrafish and human cardiomyocytes significantly increased ROS production compared with the cardiomyocytes treated with vehicle. Our results suggest that induction of ROS by sorafenib in zebrafish and human cardiomyocytes is associated with reduction of *STC1*.

STC1 is a glycoprotein hormone involved in calcium/phosphate homeostasis, which was originally discovered as a secretory hormone of the corpuscle of Stannius, an endocrine gland of teleosts (Jiang *et al.*, 2000). This gene is evolutionarily highly conversed, with the first 202 amino acids showing 90% similarity between human *STC1* (NM-003155) and zebrafish *stc1* (NM-001045457). Consequently the molecular function is also highly conserved in vertebrates, including fish (Ishibashi and Imai, 2002). In addition, mammalian *STC1* is widely expressed in various tissues including the heart (Guo *et al.*, 2013; Yeung *et al.*, 2012), similar to zebrafish in this study. Clinically, *STC1* is upregulated in the hearts of patients with myocardial infarction and idiopathic dilated cardiomyopathy (Guo *et al.*, 2013). However, it remains unclear whether downregulation of *STC1* by sorafenib treatment is associated with ROS generation in cardiomyocytes as a mechanism of cardiotoxicity of sorafenib.

Liu *et al.* have reported that human *STC1* activates a novel antioxidant pathway in cardiomyocytes through induction of uncoupling protein 3 UCP3, suggesting that *STC1* plays an important role in suppressing ROS in the heart (Liu *et al.*, 2012). In our study, reduction of *STC1* activated ROS production in human cardiomyocytes. Nguyen *et al.* also have reported that the expression of *stc1* is positively regulated by ERK signaling (Nguyen *et al.*, 2009). Therefore, sorafenib might induce overproduction of ROS caused by *STC1* downregulation, through inhibition of ERK signaling, resulting in cytotoxic effects in both zebrafish heart and human cardiomyocytes.

Finally, we performed forced expression of *stc1* to rescue the ventricular dysfunction in zebrafish treated with sorafenib. To normalize expression level of *stc1* in zebrafish treated with sorafenib, we injected *stc1* mRNA into zebrafish eggs and then treated them with 1 μM sorafenib from 72 to 96 hpf. We found that the forced expression of *stc1* in zebrafish with sorafenib treatment normalized the decreasing longitudinal ventricular dimensions caused by sorafenib treatment. Consequently, these studies suggest that *STC1* plays a role in protection against oxidative stress by ROS overproduction in cardiomyocytes following sorafenib treatment.

In conclusion, we established that *STC1* downregulation is responsible for sorafenib-induced cardiotoxicity through activated ROS generation.

SUPPLEMENTARY DATA

Supplementary data are available online at http://toxsci.oxfordjournals.org/.

FUNDING

This work was supported in part by grants from Mie University Graduate School of Medicine; the Ministry of Education, Culture, Sports, Science and Technology (MEXT) of Japan; the Japan Science and Technology Agency; the Long-range Research Initiative of the Japan Chemical Industrial Association (2010NT02, 2011NT02-01); the Johns Hopkins Center for Alternatives to Animal Testing (2011-08, 2012-17); and the Sumitomo Foundation (113498).

ACKNOWLEDGMENTS

We express our gratitude to Dr K. Dohi and Dr K. Miyashita for helpful discussions, and T. Oka for teaching us bioinformatics analysis. We are grateful to Dr K. Kawakami (National Institute of Genetics, Japan) for providing the SAG4A line. We thank R. Kawase, S. Ichikawa, M. Ariyoshi, H. Nakayama and J. Koiwa for zebrafish breeding, and R. Ikeyama and Y. Tamura for secretarial assistance.

REFERENCES

Adão, R., de Keulenaer, G., Leite-Moreira, A., and Brás-Silva, C. (2013). Cardiotoxicity associated with cancer therapy: Pathophysiology and prevention strategies. *Rev. Port. Cardiol.* **32,** 395–409.

Berthiaume, J. M., and Wallace, K. B. (2007). Adriamycin-induced oxidative mitochondrial cardiotoxicity. *Cell Biol. Toxicol.* **23,** 15–25.

Bruix, J., Sherman, M., American Association for the Study of Liver Diseases. (2011). Management of hepatocellular carcinoma: An update. *Hepatology* **53,** 1020–1022.

Burns, C. G., and MacRae, C. A. (2006). Purification of hearts from zebrafish embryos. *Biotechniques* **40,** 274–278.

Cheng, A. L., Kang, Y. K., Chen, Z., Tsao, C. J., Qin, S., Kim, J. S., Luo, R., Feng, J., Ye, S., Yang, T. S., *et al.* (2009). Efficacy and safety of sorafenib in patients in the Asia-Pacific region with advanced hepatocellular carcinoma: A phase III randomised, double-blind, placebo-controlled trial. *Lancet Oncol.* **10,** 25–34.

Cheng, H., Kari, G., Dicker, A. P., Rodeck, U., Koch, W. J., and Force, T. (2011). A novel preclinical strategy for identifying cardiotoxic kinase inhibitors and mechanisms of cardiotoxicity. *Circ. Res.* **109,** 1401–1409.

Chiou, J. F., Tai, C. J., Wang, Y. H., Liu, T. Z., Jen, Y. M., and Shiau, C. Y. (2009). Sorafenib induces preferential apoptotic killing of a drug- and radio-resistant Hep G2 cells through a mitochondria-dependent oxidative stress mechanism. *Cancer Biol. Ther.* **8,** 1904–1913.

Collins, T. J. (2007). ImageJ for microscopy. *Biotechniques* **43,** 25–30.

Coriat, R., Nicco, C., Chéreau, C., Mir, O., Alexandre, J., Ropert, S., Weill, B., Chaussade, S., Goldwasser, F., and Batteux, F. (2012). Sorafenib-induced hepatocellular carcinoma cell death depends on reactive oxygen species production in vitro and in vivo. *Mol. Cancer Ther.* **11,** 2284–2293.

Di Salvo, G., Di Bello, V., Salustri, A., Antonini-Canterin, F., La Carrubba, S., Materazzo, C., Badano, L., Caso, P., Pezzano, A., Calabrò, R., *et al.* (2011). The prognostic value of early left ventricular longitudinal systolic dysfunction in asymptomatic subjects with cardiovascular risk factors. *Clin. Cardiol.* **34,** 500–506.

Feng, X., Sun, T., Bei, Y., Ding, S., Zheng, W., Lu, Y., and Shen, P. (2013). S-nitrosylation of ERK inhibits ERK phosphorylation and induces apoptosis. *Sci. Rep.* **3,** 1814.

Force, T., and Kolaja, K. L. (2011). Cardiotoxicity of kinase inhibitors: The prediction and translation of preclinical models to clinical outcomes. *Nat. Rev. Drug Discov.* **10,** 111–126.

Force, T., Krause, D. S., and Van Etten, R. A. (2007). Molecular mechanisms of cardiotoxicity of tyrosine kinase inhibition. *Nat. Rev. Cancer* **7,** 332–344.

Fumarola, C., Caffarra, C., La Monica, S., Galetti, M., Alfieri, R. R., Cavazzoni, A., Galvani, E., Generali, D., Petronini, P. G., and Bonelli, M. A. (2013). Effects of sorafenib on energy metabolism in breast cancer cells: Role of AMPK-mTORC1 signaling. *Breast Cancer Res. Treat.* **141,** 67–78.

Guo, F., Li, Y., Wang, J., and Li, G. (2013). Stanniocalcin1 (STC1) inhibits cell proliferation and invasion of cervical cancer cells. *PLoS One* **8,** e53989.

Hasinoff, B. B., and Patel, D. (2010). Mechanisms of myocyte cytotoxicity induced by the multikinase inhibitor sorafenib. *Cardiovasc. Toxicol.* **10,** 1–8.

Holmes, D. I., and Zachary, I. C. (2008). Vascular endothelial growth factor regulates stanniocalcin-1 expression via neuropilin-1-dependent regulation of KDR and synergism with fibroblast growth factor-2. *Cell Signal* **20,** 569–579.

Ishibashi, K., and Imai, M. (2002). Prospect of a stanniocalcin endocrine/paracrine system in mammals. *Am. J. Physiol. Renal Physiol.* **282,** F367–F375.

Jacob, E., Drexel, M., Schwerte, T., and Pelster, B. (2002). Influence of hypoxia and of hypoxemia on the development of cardiac activity in zebrafish larvae. *Am. J. Physiol. Regul. Integr. Comp. Physiol.* **283,** R911–R917.

Jiang, W. Q., Chang, A. C., Satoh, M., Furuichi, Y., Tam, P. P., and Reddel, R. R. (2000). The distribution of stanniocalcin 1 protein in fetal mouse tissues suggests a role in bone and muscle development. *J. Endocrinol.* **165,** 457–466.

Kawakami, K., Takeda, H., Kawakami, N., Kobayashi, M., Matsuda, N., and Mishina, M. (2004). A transposon-mediated gene trap approach identifies developmentally regulated genes in zebrafish. *Dev. Cell* **7,** 133–144.

Koizumi, K., Hoshiai, M., Ishida, H., Ohyama, K., Sugiyama, H., Naito, A., Toda, T., Nakazawa, H., and Nakazawa, S. (2007). Stanniocalcin 1 prevents cytosolic $Ca2+$ overload and cell hypercontracture in cardiomyocytes. *Circ. J.* **71,** 796–801.

Lal, H., Kolaja, K. L., and Force, T. (2013). Cancer genetics and the cardiotoxicity of the therapeutics. *J. Am. Coll. Cardiol.* **61,** 267–274.

Lister, J. A., Robertson, C. P., Lepage, T., Johnson, S. L., and Raible, D. W. (1999). Nacre encodes a zebrafish microphthalmia-related protein that regulates neural-crest-derived pigment cell fate. *Development* **126,** 3757–3767.

Liu, D., Huang, L., Wang, Y., Wang, W., Wehrens, X. H., Belousova, T., Abdelrahim, M., DiMattia, G., and Sheikh-Hamad, D. (2012). Human stanniocalcin-1 suppresses angiotensin II-induced superoxide generation in cardiomyocytes through UCP3-mediated anti-oxidant pathway. *PLoS One* **7,** e36994.

Llovet, J. M., Di Bisceglie, A. M., Bruix, J., Kramer, B. S., Lencioni, R., Zhu, A. X., Sherman, M., Schwartz, M., Lotze, M., Talwalkar, J., *et al.* (2008a). Design and endpoints of clinical trials in hepatocellular carcinoma. *J. Natl Cancer Inst.* **100,** 698–711.

Llovet, J. M., Ricci, S., Mazzaferro, V., Hilgard, P., Gane, E., Blanc, J. F., de Oliveira, A. C., Santoro, A., Raoul, J. L., Forner, A., *et al.* (2008b). Sorafenib in advanced hepatocellular carcinoma. *N. Engl. J. Med.* **359,** 378–390.

Mellor, H. R., Bell, A. R., Valentin, J. P., and Roberts, R. R. (2011). Cardiotoxicity associated with targeting kinase pathways in cancer. *Toxicol. Sci.* **120,** 14–32.

Miyahara, K., Nouso, K., and Yamamoto, K. (2014). Chemotherapy for advanced hepatocellular carcinoma in the sorafenib age. *World J. Gastroenterol.* **20,** 4151–4159.

Nguyen, A., Chang, A. C., and Reddel, R. R. (2009). Stanniocalcin-1 acts in a negative feedback loop in the prosurvival ERK1/2 signaling pathway during oxidative stress. *Oncogene* **28,** 1982–1992.

Ogrunc, M., Di Micco, R., Liontos, M., Bombardelli, L., Mione, M., Fumagalli, M., Gorgoulis, V. G., and d'Adda di Fagagna, F. (2014). Oncogene-induced reactive oxygen species fuel hyperproliferation and DNA damage response activation. *Cell Death Differ.* **21,** 998–1012.

Orphanos, G. S., Ioannidis, G. N., and Ardavanis, A. G. (2009). Cardiotoxicity induced by tyrosine kinase inhibitors. *Acta Oncol.* **48,** 964–970.

Roux, P. P., and Blenis, J. (2004). ERK and p38 MAPK-activated protein kinases: A family of protein kinases with diverse biological functions. *Microbiol. Mol. Biol. Rev.* **68,** 320–344.

Schmidinger, M., Zielinski, C. C., Vogl, U. M., Bojic, A., Bojic, M., Schukro, C., Ruhsam, M., Hejna, M., and Schmidinger, H. (2008). Cardiac toxicity of sunitinib and sorafenib in patients with metastatic renal cell carcinoma. *J. Clin. Oncol.* **26,** 5204–5212.

Seguchi, O., Takashima, S., Yamazaki, S., Asakura, M., Asano, Y., Shintani, Y., Wakeno, M., Minamino, T., Kondo, H., Furukawa, H., *et al.* (2007). A cardiac myosin light chain kinase regulates sarcomere assembly in the vertebrate heart. *J. Clin. Investig.* **117,** 2812–2824.

Strumberg, D., Clark, J. W., Awada, A., Moore, M. J., Richly, H., Hendlisz, A., Hirte, H. W., Eder, J. P., Lenz, H., and Schwartz, B. (2007). Safety, pharmacokinetics, and preliminary antitumor activity of sorafenib: A review of four phase 1 trials in patients with advanced refractory solid tumors. *Oncologist*, **12,** 426–437.

Tolcher, A. W., Appleman, L. J., Shapiro, G. I., Mita, A. C., Cihon, F., Mazzu, A., and Sundaresan, P. R. (2011). A phase I open-label study evaluating the cardiovascular safety of sorafenib in patients with advanced cancer. *Cancer Chemother. Pharmacol.* **67,** 751–764.

Umemoto, N., Nishimura, Y., Shimada, Y., Yamanaka, Y., Kishi, S., Ito, S., Okamori, K., Nakamura, Y., Kuroyanagi, J., Zhang, Z., *et al.* (2013). Fluorescent-based methods for gene knockdown and functional cardiac imaging in zebrafish. *Mol. Biotechnol.* **55,** 131–142.

Westerfield, M. (2007). *The Zebrafish Book, a Guide for the Laboratory Use of Zebrafish (Danio rerio)*, 4th ed. University of Oregon Press, Eugene, OR.

Yeung, B. H., Law, A. Y., and Wong, C. K. (2012). Evolution and roles of stanniocalcin. *Mol. Cell Endocrinol.* **349,** 272–280.